Application of Wavelet and Regression Analysis in Assessing Temporal and Geographic Climate Variability: Eastern Ontario, Canada as a Case Study

Andreas Prokoph[1*] and R. Timothy Patterson[2]

[1]*SPEEDSTAT, 36 Corley Private, Ottawa, ON, K1V 8T7*
[2]*Department of Earth Sciences and Ottawa-Carleton Geoscience Centre, Herzberg Building, Carleton University, Ottawa, ON*

[Original manuscript received 10 November 2003; in revised form 23 April 2004]

ABSTRACT *Regression and wavelet analysis have been employed to trace and quantify variation in temporal patterns (e.g., cycles and trends) between the instrument climate records of urban Ottawa and nearby rural areas in eastern Ontario. Possible links between observed climate change at these stations and possible natural and anthropogenic drivers were also investigated. Regression analysis indicates that the temperature in Ottawa increased, on average, at a rate of >0.01°C yr^{-1} in comparison to adjacent rural areas over the last century. Wavelet analysis shows that this relative urban warming trend was primarily manifested in the form of multi-decadal and interseasonal cycles that are likely attributable to gradual increased winter heating in Ottawa (heat island effects) associated with population growth. We estimate that the 1°C increase in the Ottawa temperature is equivalent to an increase in population size of ~400,000. In contrast, interannual variability correlates well between rural and urban areas with about the same temperature amplitudes.*

RÉSUMÉ *[traduit par la rédaction] On a utilisé l'analyse de la régression et des ondelettes pour discerner et quantifier la variation dans les configurations temporelles (p. ex., cycles et tendances) entre les relevés climatologiques instrumentaux dans la région urbaine d'Ottawa et dans la région rurale avoisinante de l'Est de l'Ontario. On étudie aussi les liens possibles entre le changement climatique observé à ces stations et d'éventuelles causes naturelles ou anthropiques. L'analyse de régression indique que, durant le dernier siècle, la température, à Ottawa, a augmenté à un rythme annuel moyen supérieur à 0,01 °C, par comparaison aux régions rurales adjacentes. L'analyse des ondelettes montre que cette tendance au réchauffement urbain relatif s'est principalement manifestée sous la forme de cycles multidécennaux et intersaisonniers vraisemblablement attribuables à une augmentation du chauffage en hiver à Ottawa (effets d'îlot de chaleur), augmentation liée à l'accroissement démographique. Nous estimons que l'augmentation de température de 1 °C à Ottawa équivaut à un accroissement de la taille de la population de ~400 000. Par contraste, la variabilité interannuelle est bien corrélée entre les régions rurales et urbaines, avec à peu près les mêmes amplitudes de température.*

1 Introduction

Statistical analysis of worldwide observational temperature records has revealed a global temperature increase of 0.3°–0.7°C over the last century (IPCC, 1996). In the northern hemisphere most of this increase has been attributed to a decrease in diurnal temperature range, suggesting that conditions are actually 'less cold' rather than 'warmer' (e.g., Bonsal et al., 2001). This warming has alternatively been linked to an increase in anthropogenic greenhouse gas CO_2 output (IPCC, 1996), a growing urban heat island effect as North American urban centres have grown in size (Karl et al., 1988), or natural processes such as changes in solar radiation (e.g., Carslaw et al., 2002).

Urban heat islands are the result of numerous anthropogenic heat sources, decreased evapotranspiration related to construction material heat storage, and a decrease in longwave radiation loss due to a reduction in sky view factors (e.g., Oke, 1982; Gallo et al., 1996, 1999). Temperature increases due to the heat island effect vary with the square root of

*Corresponding author's e-mail: aprokocon@aol.com

population size, varying from 0.06°C for a population of ~2,000 to ~0.7°C for a population of 500,000 (Karl et al., 1988). Thus, temperature variability, including long-term trends, recorded in, or near, urban centres is not necessarily representative of global or even regional temperature changes (e.g., Quereda Sala et al., 2000). It has been estimated that southern Canada warmed between 0.5° and 1.5°C during the twentieth century due to several sources of anthropogenic warming, including greenhouse gases (Bonsal et al., 2001; Zhang et al., 2000).

A potentially valuable tool for discriminating temporal and geographic climate variability is wavelet analysis. Wavelet analysis emerged as a filtering and data compression method in the 1980s (e.g., Morlet et al., 1982). Since then, it has been widely applied in many disciplines (e.g., Grossman and Morlet, 1984). This methodology has recently been used to trace changes in trends and cycles, rainfall variability (e.g., Nakken, 1999), solar irradiance, and interdecadal climate oscillations (e.g., Oh et al., 2002; Lucero and Rodriguez, 2000) over time. In the last decade autoregressive moving-average (ARMA) (e.g., Karl et al., 1991), 'analysis of variance' (ARIMA) (e.g., Zwiers and Kharin, 1998) and regression models (e.g., Vincent, 1998) have also been used to evaluate possible climate change scenarios and inhomogeneities within climate records. The detection of non-stationarities (i.e., interruptions or non-persistence in the temperature variability record) is particularly crucial when making statistical inferences (e.g., Katz, 1988; Bunde et al., 2001). These earlier inhomogeneity analysis models filtered out inhomogeneities as differences compared to specific trends (i.e., regressive trend) or bandwidths (i.e., by using low-pass filters utilizing moving averages, while wavelet-transform presents inhomogeneities in time series as the sum of temporal changes in the amplitude and phase of records over a wide sine-wave bandwidth.

Our objectives for this case study are to:

(1) Discriminate the variability associated with trends, cyclic components, and non-stationarities (e.g., inhomogeneities) in temperature records from eastern Ontario;
(2) Apply time-series analysis methodology to monthly temperature records, monthly records of urban-rural differences, and to records of differences in interseasonal temperature variance between urban (Ottawa) and rural areas (Morrisburg, Maniwaki) in eastern Canada;
(3) Assess whether any differences observed in temperature patterns can be linked to human influence (e.g., development of an urban heat island effect).

2 Time series analysis methods

a *Wavelet Analysis*

One approach used to understand climatic signals better (i.e., temperature records) is to extract the relevant information from a temperature time series by transforming them. The traditional way to extract periodic features is to utilize a Fourier transform. Unfortunately, the Fourier transform is limited because a single analysis window cannot detect features in the signals that are either much longer or shorter than the window size. 'Moving-window' Fourier transform (MWFT) slides a fixed-size analysis window along the time axis and is able to detect non-stationarities (e.g., Rioul and Vetterli, 1991). The fixed size window algorithm of MWFT limits the detection of cycles at wavelengths that are longer than the analysis windows, and non-stationarities in short wavelengths (i.e., high frequencies) are smoothed. Use of the wavelet transform solves this problem, because it uses narrow windows at high frequencies, and wide windows at low frequencies (Fig. 1).

Thus, wavelet analysis permits an automatic localization of objects, such as periodic-cyclic sequences, in time, space, and frequency domains including data reduction and signal filtering (e.g., Rioul and Vetterli, 1991). The features of the wavelet transform and properties of its various analysis functions ('mother wavelets') have been widely studied, and books by Kaiser (1993) and Daubechies (1992) provide an overview of the variety of different wavelet analysis techniques available.

For this time-series study, the capacity of a one-dimension al wavelet transform that will be utilized for automatic localization of periodic-signals, gradual shifts, and abrupt interruptions (discontinuities), will be exploited. The wavelet coefficients, *W,* of a time series, *x(s),* are calculated by a simple convolution:

$$W_{\psi}(a,b) = \left(\frac{1}{a}\right)\int x(s)\psi\left(\frac{s-b}{a}\right)ds \qquad (1)$$

where ψ is the mother wavelet*;* the variable *a* is the scale factor that determines the characteristic wavelength (=1/frequency); and *b* represents the shift of the wavelet over, *x(s),* (Chao and Naito, 1995). The wavelet coefficients, *W,* are normalized to represent the amplitude of Fourier frequencies.

We have utilized a continuous wavelet transform, with the Morlet wavelet as the mother function (Morlet et al., 1982). The Morlet wavelet is simply a sinusoid with a wavelength/period, *a,* modulated by a Gaussian function (Fig. 1), and has provided robust results in analyses of climate-related records (Prokoph and Barthelmes, 1996; Appenzeller et al., 1998; Gedalof and Smith, 2001).

The shifted and scaled Morlet mother wavelet is defined as:

$$\psi^{l}_{a,b}(s) = \pi^{-\frac{1}{4}}(al)^{-\frac{1}{2}} e^{-i2\pi\frac{1}{a}(s-b)} e^{-\frac{1}{2}\left(\frac{s-b}{al}\right)^2}. \qquad (2)$$

The parameter *l* addresses Heisenberg's uncertainty principle (e.g., Rioul and Vetterli, 1991) that the location and velocity of objects cannot be measured at maximum precision simultaneously. Thus *l* is used to modify the wavelet transform bandwidth-resolution either in favour of time or in favour of

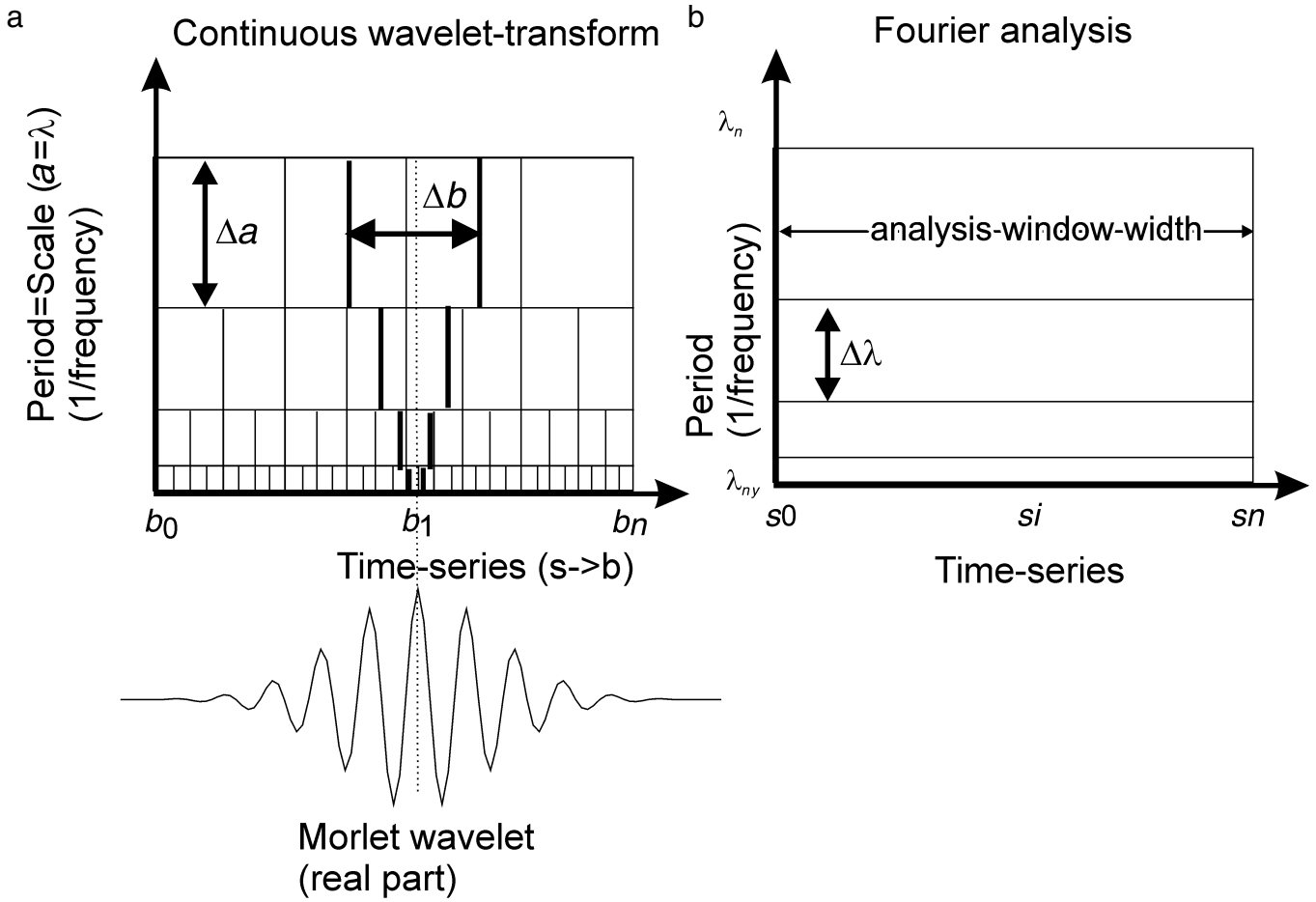

Fig. 1 Schematic presentation of analysis windows and bandwidth uncertainties for (a) continuous wavelet analysis (simplified for a dyadic wavelet) including the real part of Morlet wavelet (bottom) and region of influence of a single signal spike ($b = b1$), (b) Fourier transform.

frequency, and represents the length of the mother wavelet. The bandwidth resolution, $\Delta a/a$, for the wavelet transform varies with

$$\frac{\Delta a}{a} = \frac{\sqrt{2}}{4\pi l}, \tag{3}$$

and a location resolution $\Delta b = \frac{al}{\sqrt{2}}$. (4)

The parameter $l = 10$ is chosen for all analyses, which gives sufficiently precise results in resolving depth and frequency respectively (Prokoph and Barthelmes, 1996; Ware and Thomson, 2000). The relative bandwidth resolution, $\Delta a/a$, is, according to Eq. (3), a constant for all scales.

The wavelet coefficients at the beginning and end of the data are subject to 'edge effects', because only half of the Morlet wavelet lies inside the dataset. The missing data for the analysis window therefore have to be replaced ('padded') by zeros. For long wavelengths (e.g., wavelength a covers more than half of the whole data series), the edge effect can stretch across the entire time series. Thus, the boundary of edge effects on the wavelet coefficients forms a wavelength dependent curve for the 50% 'edge-effect free' areas known as the 'cone of influence' (Torrence and Compo, 1998).

To transform a measured, and hence limited and discrete time-series, the integral in Eq. (1) has to be modified to a numerical solution by using the trapezoidal rule for unevenly sampled points. This evaluation of the wavelet transform, provides an estimate $W^*_{l(a,b)}$ (Prokoph and Barthelmes, 1996). Visualization of the values $W^*_{l(a,b)}$ has been carried out using interpolation and coding with appropriate colours or shades of grey. In our approach, we used four shades of grey, including white and black, to represent ranges of amplitudes of the underlying sinusoidal signals. Prokoph and Barthelmes (1996) describe the method and computer program CWTA.F utilized in detail.

b *Synthetic Model*

The differences in time-frequency resolution obtained using both methods are illustrated in Fig. 2. In both cases the wavelet scalogram and periodogram obtained using a discrete

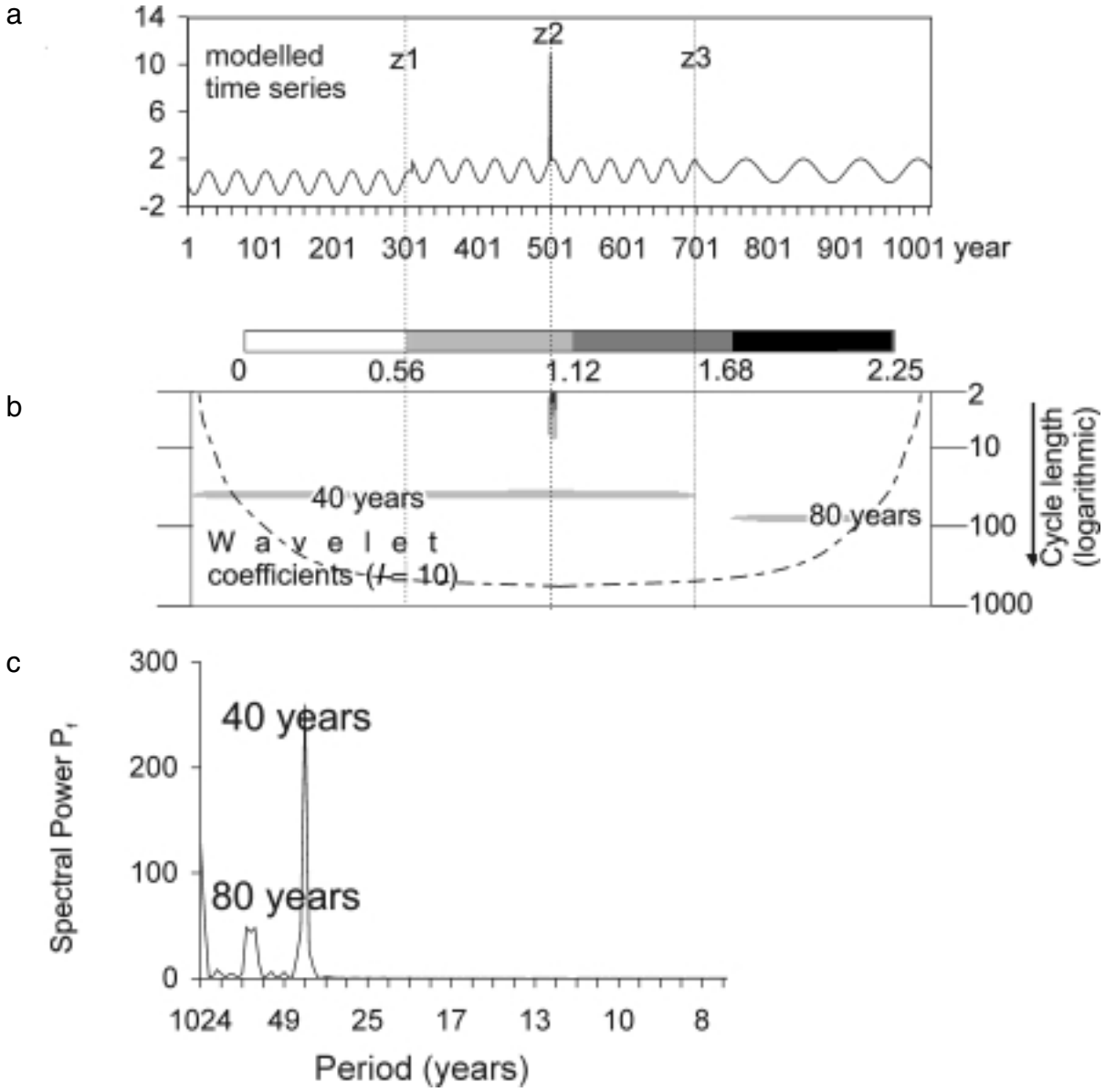

Fig. 2 Synthetic temperature record of constant amplitude with three types of abrupt changes (z1, z2, z3) in different time intervals: z1, increase of mean, z2, extreme event; z3, wavelength doubling. (a) Synthetic time-series, (b) Wavelet scalogram, the vertical axis represents the wavelength ('scales') on a logarithmic scale, the horizontal scale is time, on top: grey colour codes for wavelet coefficient which are normalized to amplitudes of a sine wave. The dark grey and black areas in the scalogram mark well-pronounced cyclicity for specific time intervals of the 1001-year record. Note that there is no significant edge effect, and the low-frequency harmonics of the periodic signals are only marginally present; (c) Periodogram of the discrete Fourier transform of the synthetic temperature record.

Fourier transform of a synthetic climatic signal with three types of inhomogenities (z1, z2, z3) are used.

The model includes three kinds of discontinuities (z1, z2 and z3), with superimposed periodic cycles at:

$x(t) = \sin(2\pi t/80)+1$	t = AD 700 to 1000
$x(t) = \sin(2\pi t/40)+1$	t = AD 300 to 699
$x(t) = \sin(2\pi t/40)+10$	t = AD 500
$x(t) = \sin(2\pi t/40)$	t = AD 1 to 300

The theoretical discontinuities z1, z2, and z3 can be expressions of the following scenarios:

1) Discontinuity z1 can be due to an abrupt jump in the mean value of the periodic signal, $x(t)$—> mean $2x(t)$, such as would occur in temperature records after a meteorological station is moved to another location, or through construction of a heat source (e.g., heating plant) nearby. In this case, the frequency and amplitude of the periodic cycle would remain unchanged (compare with the scalogram in Fig. 2b).
2) Discontinuity z2 marks a single event $x(t)$=10, that is 10 times higher than the amplitude of the periodic signal. Such an event may be related to a short-term–large-scale temperature perturbation (e.g., summer heat wave), or to

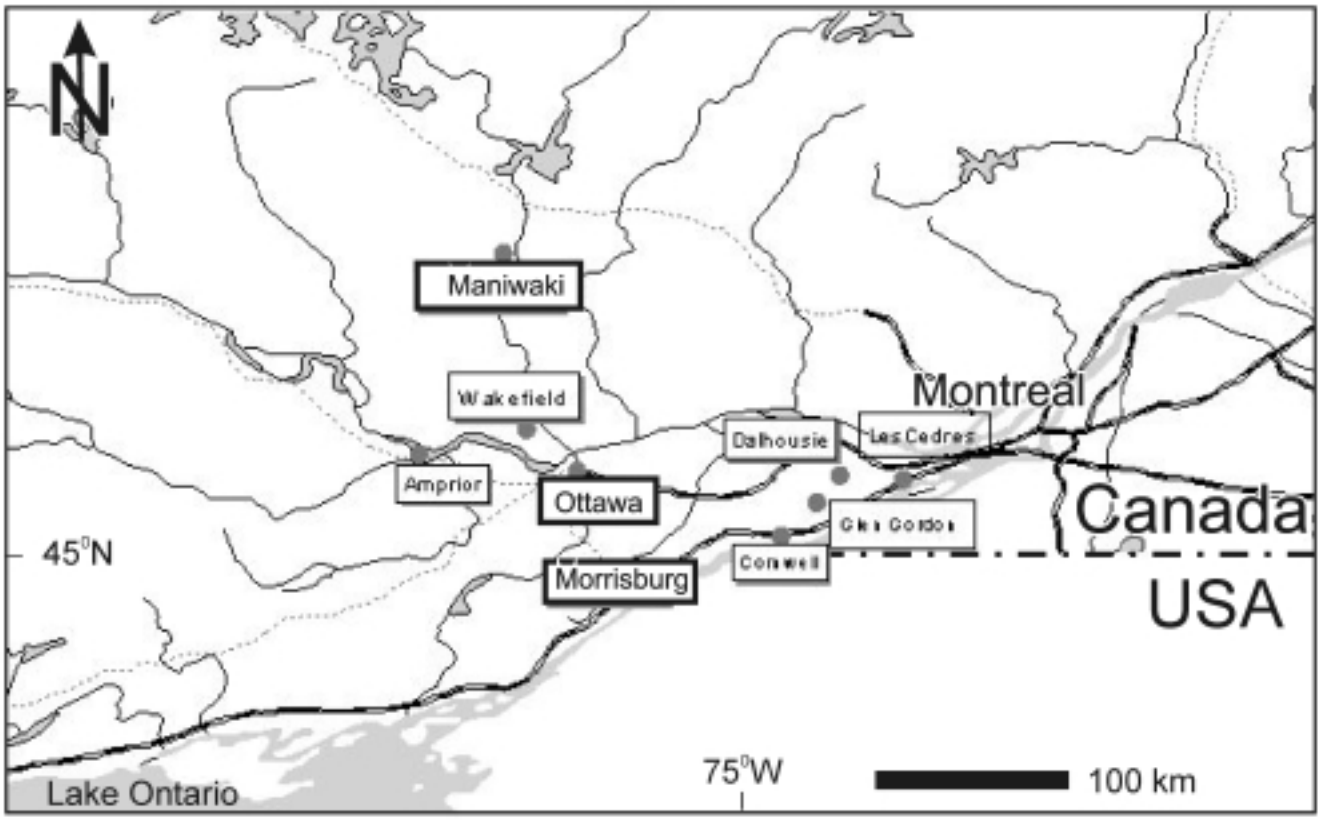

Fig. 3 Map of the Ottawa–Montreal area, eastern Canada with meteorological stations shown. Stations that were used for the study are highlighted.

a measurement error, and is detectable using both wavelet and discontinuity analysis.

3) Discontinuity z3 describes an abrupt doubling of periodicity and accumulation rate, perhaps related to changing intervals between El Niño events, and is easily detectable by wavelet analysis.

In contrast, analysis carried out using single-windowed Fourier analysis cannot be used to detect temporal discontinuities, nor can it be used to distinguish between continuous low-amplitude and non-stationary high-amplitude signals. Single-window Fourier analysis also does not yield information on the temporal persistence of periodicities (Fig. 2c).

The wavelet and spectral analysis methodology utilized for analysis of the synthetic climate record described above takes the same approach as used to analyse the actual climatic data utilized in this study.

3 Datasets

The weather station datasets utilized in this research comprise monthly averaged temperature records from mid-latitude (~45°–47°N), continental climate settings, and include records from urban Ottawa, Ontario where population growth over the last century is well documented, and shorter climate records from two rural areas; Maniwaki, Quebec, and Morrisburg, Ontario, each located approximately 100 km from Ottawa (Fig. 3). Because this study focused on an inter-annual–multidecadal cycle and long-term trend-analysis, higher-resolution data (e.g., daily averages) were not utilized. Environment Canada's Ottawa-CDA climate station, located at the central Experimental Farm, archives 113 years of data. Ottawa had a population of about 30,000 in 1890 and steadily grew to a population of ~200,000 by 1950. The city underwent intensive suburban settlement during the 1960s and had grown to ~650,000 with a metropolitan area population of ~1,000,000 by 2000. The core population of Ottawa at the time of amalgamation with several satellite cities in 2001 was 477,485 (2001 census data). The city of Ottawa has also periodically annexed other neighbouring communities over the years. To maintain consistency, suburban municipalities that were not part of the city of Ottawa in 1890 were not included in the analysis. Morrisburg, with a current population of <2,500, has an 89-year temperature record. Maniwaki, with a population of <5,000, is represented by a 40-year temperature record.

We used four types of records in the analysis:

1) Monthly normal temperature records;
2) Records of monthly normal urban–rural temperature differences.

These records are estimated by $\Delta T_{u\text{-}r} = x_i(\text{urban}) - x_i(\text{rural})$ with x representing temperature (in °C) and i coeval monthly intervals. $\Delta T_{u\text{-}r}$ is utilized for evaluation of the background variability, which is the monthly normal difference between the rural Morrisburg and Maniwaki stations (Fig. 4);

3) Annual temperature range (*ATR*) for each record. This value is estimated by:

$$ATR_i = \frac{1}{6}\sum_{j=i-6}^{j=i-1}\left|x_j - x_{j+6}\right| \quad \text{for } i = 7....N\text{-}5 \qquad (5)$$

where x represents temperature (in °C). The parameter N represents the total number of monthly data (=length of record). This record slides at 1-month intervals across the record, thus the *ATR*-record is auto-correlated over 12-month intervals. These records were not analysed using the wavelet transform. Thus, the *ATR*-record represents a bandwidth-filter for the annual cycle, but is also able to detect changes in the amplitude of this cycle over a 12-month period that is centred at specific months, i.

4) Urban-rural departure in the annual temperature range $\Delta(ATR_{u\text{-}r})$. This record is simply the difference between ATR_{urban} and ATR_{rural}, and is also calculated on a monthly basis.

The estimates of *ATR* are used for the evaluation of the temporal variability of the annual (i.e, seasonal) temperature range. The estimate of $\Delta(ATR_{u\text{-}r})$ is the residual signal after removal of regional (in both urban and rural record) temperature fluctuations and trends in the *ATR* signal. Thus, $\Delta(ATR_{u\text{-}r})$ represents local temporal influences (e.g., warming due to urbanization) on the seasonal temperature range (e.g., summer–winter contrast).

This approach is comparable to the diurnal temperature range (DTR) evaluation method used in various other studies (e.g., Gallo et al., 1999).

4 Results

a *Trends in the Temperature Records*

The three stations used in this study are located along an ~200-km north–south transect through eastern Ontario and western Quebec. In general, all monthly temperature records show a strong seasonal variation between January (coldest month) and July (warmest month) with an annual temperature amplitude, based on monthly means, of ~18.7° to 19.9°C (Table 1, Fig. 4a–4c), as is typical for continental climates at this latitude. The northernmost station (Maniwaki) is ~2.3°C cooler than Ottawa, and ~2.4°C cooler than the southernmost location (Morrisburg). Ottawa showed a warming trend of 0.0138°C yr^{-1} throughout the entire record. In contrast, the more rural Maniwaki and Morrisburg have maintained a relatively constant annual temperature profile. In particular, during the period from 1954–93 the temperature at the Ottawa-CDA station warmed by an average of ~0.01°C yr^{-1} compared to Morrisburg (cooling of ~0.01°C yr^{-1}), and an ~0.006°C yr^{-1} cooling at the Maniwaki station (Table 1).

A linear regression model $y = ax + b$, with a representing the temperature gradient per year, b the intercept with zero, x time and y the model value of the regression line, highlights the difference between urban and rural versus 'inter-rural' monthly temperature changes (Fig. 4e–4g). The relative temperature increase at Ottawa versus Morrisburg and Maniwaki is significant (represented by R^2 values) at >95% confidence for sample sizes of $n = 1068$ and $n = 468$, respectively (Fig. 4e–4g). The $\Delta T_{u\text{-}r}$ departures were particularly strong during the 1960s (most $\Delta T_{u\text{-}r}$ are above trend lines in Fig. 4e and Fig. 4f), and relatively weak during the early 1970s and mid-1980s. The population growth in the Ottawa region follows a predominantly linear growth model of ~4,000 persons per year with a slightly exponential component that suggests a growth rate of 1%–3% per year (average 2.1%: Fig. 4d). The population growth accelerated during the 1910s, 1960s and early 1990s (Fig. 4). In particular, the positive $\Delta T_{u\text{-}r}$ departure during the 1960s correlates well with intensive suburban development around the Ottawa-CDA station. In contrast the R^2 between Morrisburg and Maniwaki is insignificant.

Similar to the monthly normal temperature records, *ATR*, i.e., summer–winter contrast, decreases significantly at the Ottawa station over the entire record at a gradient of 0.0147°C yr^{-1}, but the *ATR* at Morrisburg and Maniwaki changed only insignificantly (Figs 5a–5c). The urban–rural contrast in the annual temperature range $ATR_{u\text{-}r}$ is even more significant (Fig. 5d and Fig. 5e), while the inter-rural *ATR* differences in the records of eastern Canada are insignificant. In particular, the decrease in the $\Delta(ATR_{u\text{-}r})$ of 0.017°C yr^{-1} between Ottawa and Morrisburg (Fig. 5d) is larger than the entire warming trend at Ottawa compared with Morrisburg (Table 1). Consequently, the winter in Ottawa became milder compared to Morrisburg.

b *Results of Wavelet Analysis*

While regression analysis (see above) can describe general trends and their significance, wavelet and discontinuity analysis can be used to show the path of these trends over time, including the timing of non-stationary high-frequency cycles and abrupt changes.

Wavelet analysis of the temperature record focused on wavelengths >1.5 yr, because the strong continental seasonal contrast of >18°C (Table 1) masks all shorter wavelength cycles. All records are characterized by two major patterns: (a) trends defined by wavelengths that are longer than half of the available record length, and (b) non-stationary high-frequency cycles <12 yr. The trend can be separated into two predominant bands. The maximum available temporal wavelengths for the Ottawa and Morrisburg stations, ~225 yr and 176 yr respectively, have amplitudes of >0.8°. Thus, most of the temperature gradients for Morrisburg and Ottawa are indeed linear trends and not composite cycles (Table 1). Higher-frequency signals are correlated through all sections, and thus occur independently of local trends. In particular, wavelet analysts permits recognition of four distinct temperature regimes, separated by abrupt transitions (Fig. 6a–6c), in the last century:

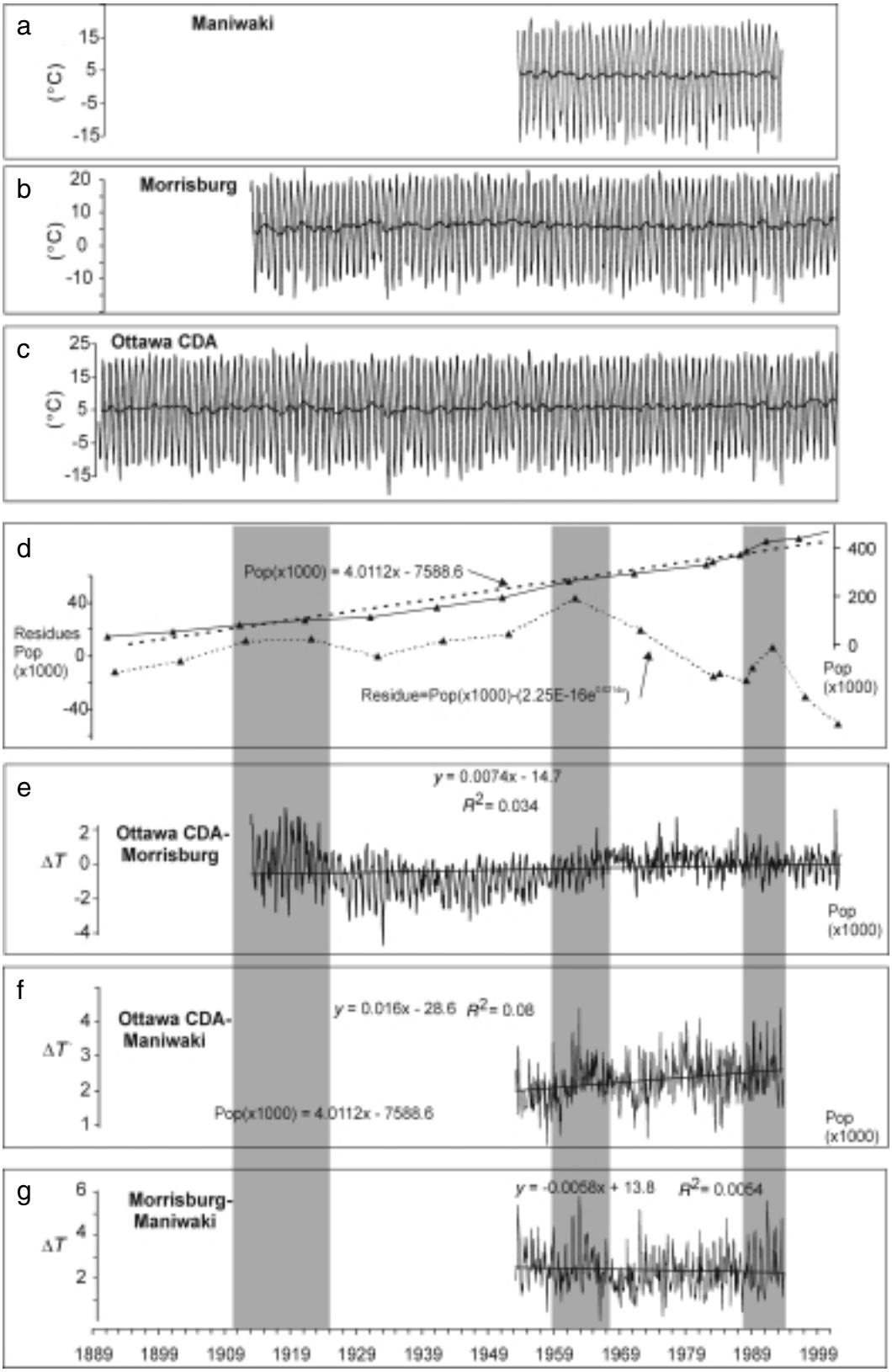

Fig. 4 (a)–(c): Monthly mean temperature records of three stations in eastern Canada with 12-month running means, note the strong seasonal variability which is much stronger than the longer-term variability; (d): Population of Ottawa Central (solid line) at 16 counts (black triangles). Lower dashed line marks residues of an exponential growth model (scale on left) and upper straight dashed line shows linear growth model (scale on right); (e)–(g): temperature difference records between urban and rural and between rural areas, and linear regression lines with equation and squared uncertainty of regression. Grey shaded boxes mark intervals of increased rate of population growth for correlation with the temperature difference records.

TABLE 1. Means, gradients and amplitudes of temperature trends in eastern Canada

	Morrisburg 1954–93	Morrisburg 1913–2002	Ottawa-CDA 1954–93	Ottawa-CDA 1889–2002	Maniwaki UA 1954–93
Mean (°C)	6	6.2	5.9	5.7	3.6
Gradient (°C yr^{-1})	–0.0117	0.0096	0.0098	0.0138	–0.0059
Annual Amplitude (°C)	18.8	18.7	19.5	19.9	19.6

(a) ~1890–1937: Highly variable non-periodic cyclic patterns that are characterized by the short-term influence of temperature cycles with fluctuating wavelengths;
(b) ~1937–71: Low temperature variability with a stationary periodic biannual cyclicity;
(c) ~1971–89: Low temperature variability and non-periodic fluctuations limited to high-frequency cycles of < 2 yr wavelengths; and
(d) Since 1989: Highly variable cyclic pattern of 1.8-, ~3.8- and 1-yr wavelengths similar to the pattern observed in regime (a) (Fig. 6c).

The temperature difference between urban and rural areas $\Delta T_{u\text{-}r}$ is the most important record when attempting to distinguish between global/regional climate variability and urban heat island effects (e.g., Gallo et al., 1999). Wavelet analysis of these records in the Ottawa area (Fig. 7) indicates that:

(a) The largest $\Delta T_{u\text{-}r}$ occur in the annual waveband with amplitudes > 0.6°C, but also in the inter-rural differences (Fig. 7c). Thus this change cannot be related to the heat island effect but rather to a decline in seasonal temperature contrast (Table 1) at Morrisburg. Wavelet analysis shows that the differences in the annual variability at Morrisburg were slightly reduced to 0.2°–0.6°C in all ΔT records from ~1965–88 (Fig. 7a–7c).
(b) Wavelet coefficients representing a >0.2°C amplitude occur in the trend range in both $\Delta T_{u\text{-}r}$ and $\Delta T_{r\text{-}r}$ (Fig. 7). According to the results of the linear regression analysis the different components in the Ottawa–Maniwaki records add up to a significant positive trend, while the trend components in the Morrisburg–Maniwaki records cancel each other out (Fig. 4f and Fig. 4g).

The analyses above indicate that the differences in the annual temperature range $\Delta(ATR_{u\text{-}r})$ are most prominent when comparing the urban and rural stations. This interseasonal variability is typical of the continental climate that characterized much of Canada (e.g., Zwiers and Kharin, 1998).

Wavelet analysis was also used to investigate signal persistence and variability in $\Delta(ATR_{u\text{-}r})$ in the region (Fig. 8). The major contribution to the variability in both $\Delta(ATR_{u\text{-}r})$ and $\Delta(ATR_{r\text{-}r})$ are non-periodic, non-persistent, and non-correlative signals with wavelengths varying between 2 and 16 years (Fig. 8a–8c). There is no particular periodic component that contributes to the diminished $\Delta T_{u\text{-}r}$ for the 1965–88 records (Fig. 7). The $\Delta(ATR_{u\text{-}r})$ in the trend waveband between Ottawa and Morrisburg shows a strong variability of >0.18°C per wavelength (Fig. 8b). In addition, all $\Delta(ATR_{u\text{-}r})$ records have a discontinuity in the cycle pattern that is centred about 8/1979 (Fig. 8).

5 Discussion

a *Urban Heat Island Effect*

Our results are consistent with previous research that has shown that eastern Canada has warmed by ~1°C over the last century (e.g., Bonsal et al., 2001). Unfortunately, the longest running meteorological stations in Canada are located in urban centres (e.g., Zhang et al., 2000). Linear regression analysis determined that the urban Ottawa-CDA station warmed significantly compared to the rural areas at Morrisburg and Maniwaki stations. The mean temperature in Ottawa has gradually departed by ~2°C per century from that measured in the surrounding rural areas where no significant warming trend was observed. There is an approximately linear trend in both temperature (Fig. 4e and Fig. 4f, Table 1) and population increase in the Ottawa area (Fig. 4d) relative to the surrounding rural area. We estimate that an increase of 250,000–500,000 in population can be linked to an ~1°C urban heat island effect temperature increase (average: 400,000 persons per 1°C: Fig. 4d–4f). Similar urban/rural temperature record departures have also been documented in the United States (e.g., Karl et al., 1988). Unfortunately, the uncertainty in our heat island effect estimate is high and cannot be fully evaluated at this point, because the data do not fully incorporate population growth related to many incremental urban amalgamations that have occurred over the years, as well as the uneven city growth that has taken place around the meteorological station.

Our climate analysis confirms that the departure of the Ottawa urban heat island temperature record from that documented in the rural stations resulted from a lowering of the seasonal amplitude. This provides clear evidence that the winter months in Ottawa are now relatively warmer, rather than the summer months being warmer. This result is consistent with the outcome of urban heat island effect studies elsewhere where decreases in diurnal and annual temperature variability in a city have been determined to be the result of: (a) increased night temperatures (e.g., Karl et al., 1988; Bonsal et al., 2001), and (b) relatively warmer winters, probably due to strong winter heating in urban areas.

The deviation between the urban and rural temperature trends is not linear though. Increased rates of temperature departure between rural and urban areas observed in the late 1910s, 1960s, and to a lesser degree in the early 1990s, coinciding with an increase in urban development provide the most probable explanation (Fig. 4d–4e).

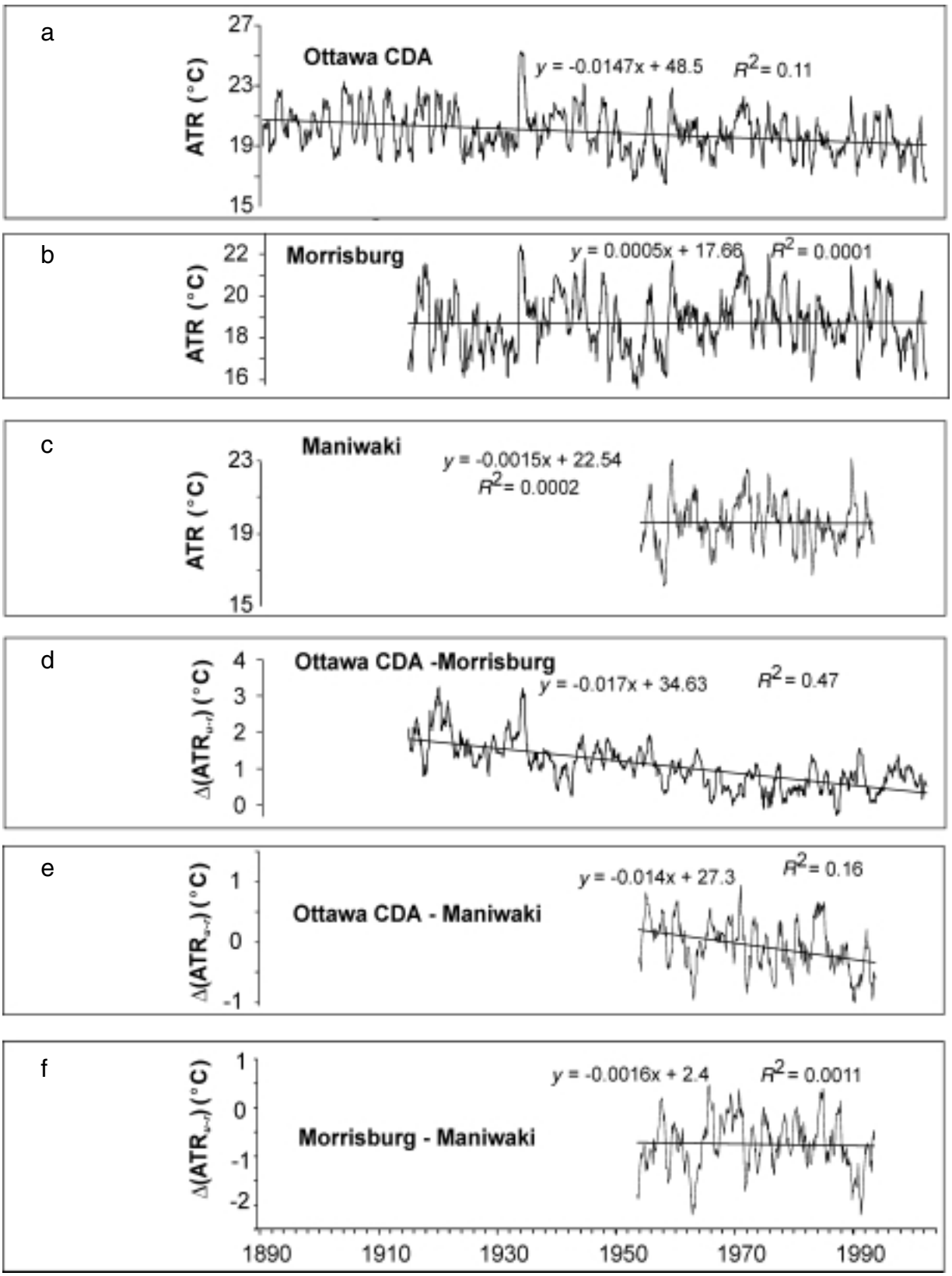

Fig. 5 (a)–(c): Annual temperature range calculated from monthly mean temperature records of three stations in eastern Canada including linear regression lines with equation and squared uncertainty (R^2) of regression. Note that only the trend for the Ottawa-CDA station is significant at >95% confidence; (d)–(f) Urban–rural and rural–rural differences in annual temperature range (ATR_{u-r}), including linear regression lines with equation and squared uncertainty (R^2) of regression. Note that the *ATR* for Ottawa dropped significantly compared to the rural areas but the differences between rural areas changed insignificantly.

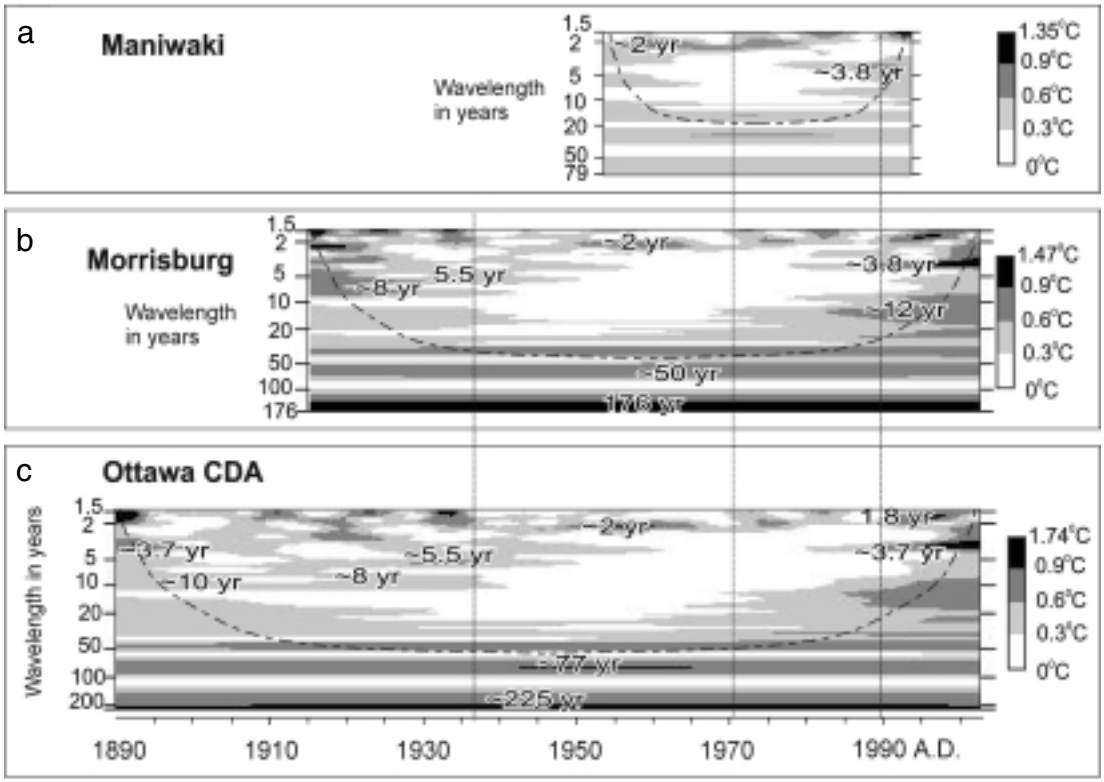

Fig. 6 Wavelet analysis (for wavelengths >1.5 yr) of three temperature records in eastern Canada: (a): Maniwaki; (b): Ottawa-CDA; and (c): Morrisburg. For a–c: Wavelet scalograms with 'cone of influence' and marking of major wavelet coefficients (for details see text), right sides: grey-scale coded wavelet coefficient ranges; Vertical dotted lines: Correlations aid for discontinuities in the wavelet pattern.

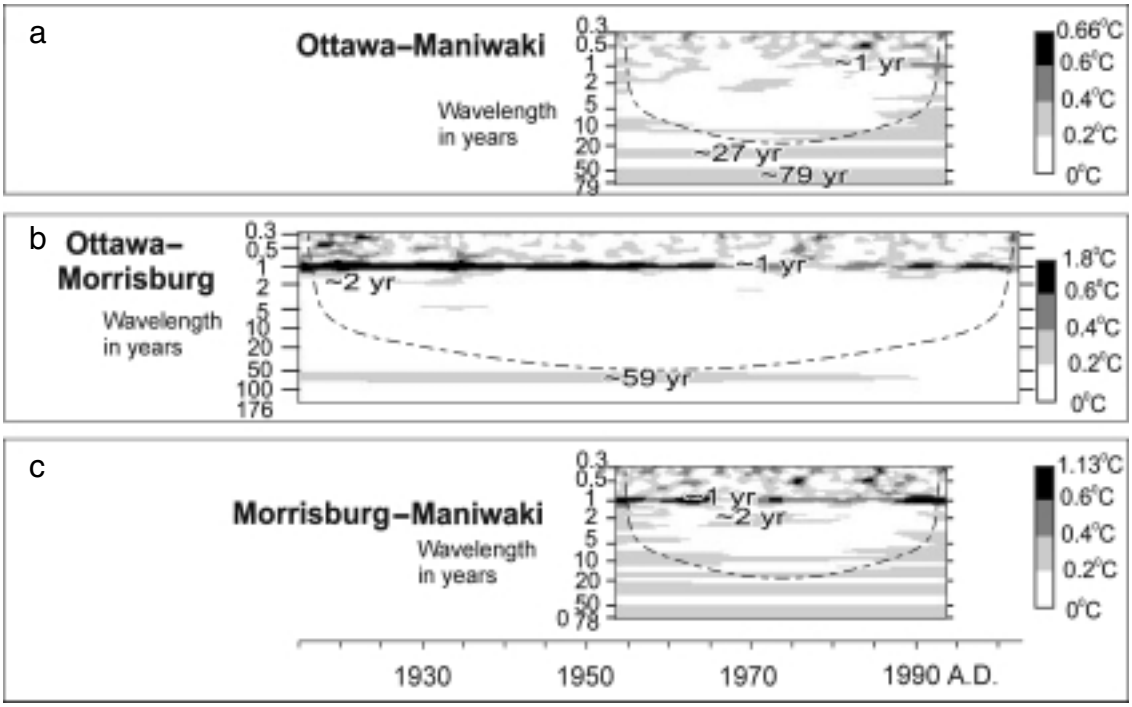

Fig. 7 Wavelet analysis (for wavelengths >0.3 year = ~4 months) of three (a–c) records of urban–rural (a+b) and rural–rural (c) monthly normal temperature differences in eastern Canada: For a–c: Wavelet scalograms with 'cone of influence' and marking of major wavelet coefficients (for details see text), right sides: grey-scale coded wavelet coefficient ranges.

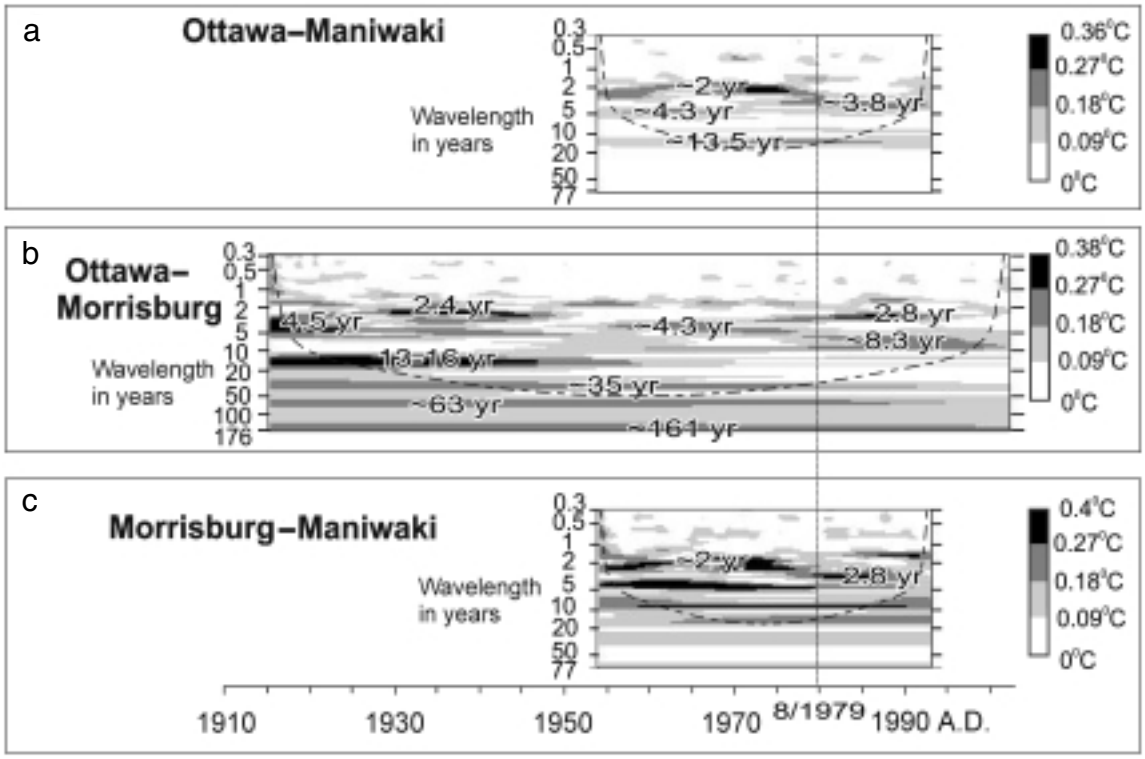

Fig. 8 Wavelet analysis (for wavelengths >0.3 year = ~4 months) of three (a–c) records of urban-rural (a+b) and rural-rural (c) Annual temperature range difference records in eastern Canada: For a–c: Wavelet scalograms with 'cone of influence' and marking of major wavelet coefficients (for details see text), right sides: grey-scale coded wavelet coefficient ranges; Vertical dotted line: Correlations aid for discontinuities in the wavelet pattern centred about August 1979.

b *Climate Cycles in Eastern Ontario*

A combination of regression and wavelet analysis shows that much of the observed temperature increase can be attributed to long-term trends. Major contributors to the differences between the studied urban and rural stations are embedded: (a) in the annual temperature range changes $\Delta(ATR_{u\text{-}r})$ and $\Delta(ATR_{u\text{-}r})$, and (b) in the long-term trend and interdecadal cyclicity. $\Delta(ATR_{u\text{-}r})$ and $\Delta(ATR_{r\text{-}r})$ change non-periodically, mostly in 2–16-year intervals. In particular, the general decreasing trend in $\Delta(ATR_{u\text{-}r})$, for the Ottawa–Maniwaki records is a combination of different non-stationary cycles, rather than the result of any persistent linearity. Thus, because the current temperature records of the region are short, these $\Delta(ATR_{u\text{-}r})$ changes cannot be associated with the urban heat island effect.

As the climate records are so short it is also difficult to determine whether or not recognizable long-term trends are due to anthropogenic effects, or natural causes. Long-term cycles determined by wavelet analysis are influenced by 'edge effect' (Fig. 6–Fig. 8) and low bandwidth resolution (see Fig. 1) and will not be discussed further.

Wavelet analysis demonstrates that most of the short-term annual temperature range variability at each station can be attributed to non-stationary, thus poorly predictable, cycles in the 2–16-year wavelength bands. The good correlation (Fig. 6) between all stations for this temperature pattern indicates that regional, and not local, changes are responsible for these cycles. Thus, fluctuations in the heat island effect do not contribute to the short-term, 2–16-year, cyclicity. Some of the non-stationary cycles may be related to natural cycles, such as the El Niño-Southern Oscillation (ENSO) or ~11 year sunspot cycle (e.g., Friis-Christensen and Lassen, 1991), which has been identified in climate records from many areas (e.g., Oh et al., 2002). Most of the heat island effect is visible in winter–summer seasonal temperature variability between rural and urban areas in an annual band (Fig. 7), and through observed long-term gradual changes (Figs 4d–4g and Fig. 5).

6 Conclusions

The application of wavelet transform and regression analysis provides a linked interpretation for observed periodic cycles, trends and non-stationarities at different timescales in the climate records examined.

Our research results indicate that a significant portion of the long-term temperature record in the annual and multi-decadal spectrum in urban Ottawa is a result of episodic urbanization (i.e., heat island effects). Analysis of normalized monthly temperature records from three stations in eastern Canada indicates that there was: (a) no significant temperature increase outside the urban Ottawa area during the last century, and (b) most of the interannual variability in the urban and rural areas could be related to non-periodic natural fluctuations.

References

APPENZELLER, C.; T.F. STOCKER and M. ANKLIN. 1998. North Atlantic oscillation dynamics recorded in Greenland ice cores. *Science,* **282**: 446–449.

BONSAL, B.R.; X. ZHANG, L.A. VINCENT and W.D. HOGG. 2001. Characteristics of daily and extreme temperatures over Canada. *J. Clim.* **14**: 1959–1976.

BUNDE, A; S. HAVLIN, E. KOSCIELNY-BUNDE and H.-J. SCHELLNHUBER. 2001. Long-term persistence in the atmosphere: Global laws and tests of climate models. *Physica A: Stat. Mech. Apps.* **302**: 255–267.

CARSLAW, K.S.; R.G. HARRISON and J. KIRKBY. 2002. Cosmic rays, clouds, and climate. *Science,* **298**: 1732–1737.

CHAO, B.F. and I. NAITO. 1995. Wavelet analysis provides a new tool for studying Earth's rotation. *EOS* **76**: 161–165.

DAUBECHIES, I. 1992. *Ten lectures on wavelets*. *CBMS-NSF Regional Conference Series in Applied Mathematics, No. 61*, SIAM Press, Philadelphia, 357 pp.

FRIIS-CHRISTENSEN, E. and K. LASSEN. 1991. Length of the solar cycle: An indicator of solar activity closely associated with climate. *Science,* **254**: 698–700.

GALLO, K.P.; D.R. EASTERLING and T.C. PETERSON. 1996. The influence of land use/land cover on climatological values in the diurnal temperature range. *J. Clim.* **9**: 2941–2944.

———; T.W. OWEN, D.R. EASTERLING and P.F. JAMASON. 1999. Temperature trends of the U.S. Historical Climatology Network based on satellite-designated land use/land cover. *J. Clim.* **12**: 1344–1348.

GEDALOF, Z. and D.J. SMITH. 2001. Interdecadal climate variability and regime-scale shifts in Pacific North America. *Geophys. Res. Lett*. **28**: 1515–1518.

GROSSMAN, A. and J. MORLET. 1984. Decomposition of Hardy functions into square integrable wavelets of constant shape. *SIAM J. Math. Anal*. **15**: 732–736.

IPCC. 1996. Climate change 1995: The science of climate change. In: *Intergovernmental Panel on Climate Change*. J.T. Houghton, L.G. Miro Filho, B.A. Callander, N. Harris, A. Kattenberg and K. Maskell (Eds), Cambridge University Press, Cambridge. 572 pp.

KAISER, G. 1993. *A friendly guide to wavelets*. Birkenhaeuser Verlag, Basel, 300 pp.

KARL, T.R.; R.R. HEIM JR. and R.G. QUAYLE. 1991. The greenhouse effect in central north America: If not now, when? *Science,* **251**: 1058–1061.

———; H.F. DIAZ and G. KUKLA. 1988. Urbanization: Its detection and effect in the United States climate record. *J. Clim.* **1**: 1099–1123.

KATZ, R.W. 1988. Statistical procedures for making inferences about climate variability. *J. Clim.* **1**: 1057–1064.

LUCERO, O.A. and N.C. RODRIGUEZ. 2000. Statistical characteristics of interdecadal fluctuations in the Southern Oscillation and the surface temperature of the equatorial Pacific. *Atmos. Res.* **54**: 87–104.

MORLET, J.; G. AREHS, I, FOURGEAU and D. GIARD. 1982. Wave propagation and sampling theory. *Geophys.* **47**: 203.

NAKKEN, M. 1999. Wavelet analysis of rainfall-runoff variability isolating climatic from anthropogenic patterns. *Environ. Modelling Software* **14**: 283–295.

OH, H-S.; C.M. AMMANN, P. NAVEAU, D. NYCHKA and B.L. OTTO-BLIESNER. 2002. Muli-resolution time series analysis applied to solar irradiance and climate reconstructions. *J. Atmos. Solar-Terr. Phys.* **65**: 191–201.

OKE, T.R. 1982. The energetic basis of the urban heat island. *Q. J. R. Meteorol. Soc.* **108**: 1–24.

PROKOPH, A. and F. BARTHELMES. 1996. Detection of nonstationarities in geological time series: Wavelet transform of chaotic and cyclic sequences. *Comput. Geosci.* **22**: 1097–1108.

QUEREDA SALA, J.; A. GIL OLCINA, A. PEREZ-CUEVAS, J. OLCINA-CANTOS, A. RICO AMOROS and E. MONTON CHIVA. 2000. Climate warming in the Spanish Mediterranean: Natural trend or urban effect. *Clim. Change,* **46**: 473–483.

RIOUL, O. and M. VETTERLI. 1991. Wavelets and signal processing. *IEEE Special Mag.* pp. 14–38.

TORRENCE, C. and G.P. COMPO. 1998. A Practical guide to wavelet analysis: *Bull. Am. Meteorol. Soc*. **79**: 61–78.

VINCENT, L.A. 1998. A technique for the identification of inhomogeneities in Canadian temperature series. *J. Clim.* **11**: 1094–1104.

WARE, D.M. and R.E. THOMSON. 2000. Interannual to multidecadal timescale climate variations in the northeast Pacific. *J. Clim.* **13**: 3209–3220.

ZHANG, X. L.A. VINCENT, W.D. HOGG and A. NIITSOO. 2000. Temperature and precipitation trends in Canada during the 20th century. ATMOSPHERE-OCEAN, **38**: 395–429.

ZWIERS, F.W. and V.V. KHARIN. 1998. Intercomparison of interannual variability and potential predictability: An AMIP diagnostic project. *Clim. Dyn.* **14**: 517–528.